Life Sciences, Vol. 45, pp. 1349-1356 Pergamon Press
Printed in the U.S.A.

REGIONAL CEREBRAL GLUCOSE METABOLIC RATE IN HUMAN SLEEP ASSESSED BY POSITRON EMISSION TOMOGRAPHY

Monte S. Buchsbaum, J. Christian Gillin*, Joseph Wu, Erin Hazlett, Nancy Sicotte, Renee M. Dupont*, and William E. Bunney, Jr.

Department of Psychiatry, UC Irvine, Irvine, CA, 92717
and
*Department of Psychiatry, UC San Diego and San Diego Veterans Administration Medical Center

(Received in final form August 2, 1989)

Summary

The cerebral metabolic rate of glucose was measured during nighttime sleep in 36 normal volunteers using positron emission tomography and fluorine-18-labeled 2-deoxyglucose (FDG). In comparison to waking controls, subjects given FDG during non-rapid eye movement (NREM) sleep (primarily stages 2 and 3) showed about a 23% reduction in metabolic rate across the entire brain. This decrease was greater for the frontal than temporal or occipital lobes, and greater for basal ganglia and thalamus than cortex. Subjects in rapid eye movement (REM) sleep tended to have higher cortical metabolic rates than waking subjects. The cingulate gyrus was the only cortical structure to show a significant increase in glucose metabolic rate in REM sleep in comparison to waking. The basal ganglia were relatively more active on the right in REM sleep and symmetrical in NREM sleep.

Neither the basic neurophysiological mechanisms nor the functions of sleep are well understood at this time (1-8). Sleep may provide a time of "rest" which permits the body and brain to reduce energy expenditure, and to forestall exhaustion. Sleep, or at least sleep without the rapid eye movements (REM) typically associated with dreaming (NREM or non-REM sleep), decreases metabolic rate for both whole body (9) and brain in Rhesus monkeys (10). Prolonged sleep deprivation may have a hypermetabolic effect in rats (11). All of these findings may be consistent with the "rest theory" of sleep, i.e., sleep enforces a reduction of metabolic rate which permits restoration of brain and bodily structures and functions (12). Quantitative imaging of cerebral glucose metabolic rate is possible with positron emission tomography (PET) using 18-F-deoxyglucose (FDG). Heiss et al. (13) scanned four normal controls studied during a daytime nap following sleep deprivation; one subject reported dreaming, but standard polygraphic sleep staging was not obtained. They found relatively uniformly

0024-3205/89 $3.00 + .00

decreased glucose metabolic rate across cortical and subcortical structures in three non-dreamers, and an apparently increased rate in the one subject who reported a nightmare. Franck et al. (14) reported similar findings in two volunteers using polygraphically determined sleep measurements. In this study we have used positron emission tomography (PET) to assess regional cerebral metabolic rate in natural nighttime sleep in accommodated normal subjects with full polygraphically recorded sleep and sufficient sample size for detailed statistical analysis comparing wakefulness, NREM sleep and REM sleep.

Normal subjects were screened by medical and psychiatric interviews, review of sleep habits and medications, physical examination, and laboratory measures. A total of 48 male subjects then were screened on an accommodation night in the sleep laboratory. Mock intravenous lines (subcutaneous pediatric scalp vein needles) and arm warmers (for arteriolization of venous blood) were used to further simulate conditions on the scan night. Subjects were telephoned at home at 6:15 AM to wake them on the day preceding the scan. They were reminded not to nap or consume beverages containing caffeine and to report to the sleep lab at about 8:00 PM. Then, the IV lines were inserted in both arms and leads were attached for recording EEG, eye movements, submental EMG and EKG. Subjects then remained awake in their bedrooms reading quietly with the door closed until the schedule called for lights out at approximately their normal bedtime.

We studied individuals in NREM sleep, REM sleep, and while awake as confirmed by standard sleep criteria. For NREM sleep, subjects were infused with FDG, usually 15-25 minutes after the first K-complex or sleep spindle. For REM sleep, infusion was started as soon as the REM stage was clearly recognized with either saw-tooth EEG waves or rapid eye movements, low-voltage, mixed frequency EEG and EMG atonia. We usually studied the second or third REM period since they are longer than the first. REM and awake subjects were usually studied between 1 and 3 AM. FDG (5mCi) was administered over 1 minute. Arteriolized blood samples were drawn from the opposite arm through a 3mm tube at intervals increasing from 15 sec to 5 minutes with dead space correction for FDG quantification. Subjects were unaware of blood sampling. Awake controls were prepared exactly as the sleep subjects, with EEG leads and 10-foot IV tubes extending under the door and out of the room. The lights were turned off and subjects were instructed to remain awake and to carry out a saccadic eye movement task as a control for the REM subjects. This task was to imagine a grid of four squares with the numerals 1, 2, 3, and 4 in each square; they were then to serially look at each number at 30-second intervals. Eye movements appeared at regular intervals on the polygraph and EEG was monitored for sleep. If either sleep or absence of eye movements occurred, we knocked lightly on the bedroom door. A high degree of compliance was observed.

Of the 48 subjects, some of whom spent more than one night in the laboratory after the accommodation night, 40 received one injection of FDG; of these, 36 met the criterion of 75% or more of the first 32 minutes following FDG injection in the appropriate stage. No subject was scanned twice. The mean ages ($\pm$SD) for the REM, NREM, and Awake groups (n=12 for each) were 26.2$\pm$5.8, 26.7$\pm$8.6, and 25.3$\pm$6.6. For NREM, 11 subjects were studied during NREM #1,

and one during NREM #3. Of the first 32 minutes, they were in NREM an average of 90.6% of the first 32 minutes (Stage 1 an average of 3.3%; Stage 2, 52.9%; Stage 3, 28.7%; Stage 4, 9.0%; and awake, 6.1%). For REM, the subjects were in REM sleep an average of 88.3% of the first 32 minutes. For both REM and NREM, the percentages of time spent in the correct stage was somewhat higher for the first 16 minutes since all subjects began the uptake period in the correct stage. Six subjects were studied during REM #2, 4 during REM #3, and 2 during REM #1 (late occurring, perhaps because of a skipped first REM period). For NREM, stage 2 had appeared an average of 25±10.5 minutes before infusion.

Subjects were roused 32-45 minutes following FDG injection and then moved to the scanner. First, an individually molded, thermoplastic headholder was made for each subject to minimize head movement and to allow the subject's rapid positioning for scanning. Nine planes were obtained parallel to the canthomeatal line at 10mm increments. Patients were scanned between 45 and 120 minutes after FDG injection. The scans were performed with both shadow shields and septa shields in, a configuration with measured in-plane resolution of 7.6mm and 10.9mm resolution in the axial dimension. Typical plane counts were in the range of 500,000 to 800,000. A calculated attenuation correction and smoothing filter were used in reconstruction. The scanner was calibrated each scan night with a cylindrical phantom and compared to well counter data. Scans were transformed to glucose metabolic rate as done elsewhere (15).

Cortical regions of interest were measured using a modification of our cortical peel technique (16) and subcortical structures were assessed using stereotaxic coordinates derived from a standard neuroanatomical atlas (15). A line segment joining the center and

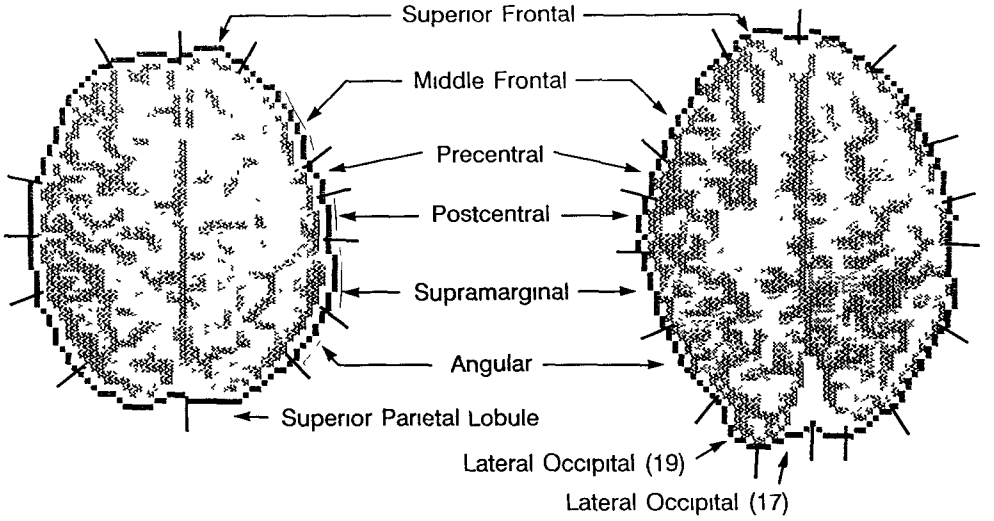

FIG. 1
Digitized atlas and computer-generated outline used to identify cortical areas. Sulcal markings were located on the original photographs.

the outline is calculated, and this line is moved radially, connecting each pixel in the outline sequentially with the center.

The area swept by the outer 2cm of this radius corresponded to the lateral cortex. The cortical strip from each hemisphere consisted of from 70 to 98 pixel values for mean metabolic rate. A similar strip of pixels was obtained by applying the peel method to a digitized photograph of the brain (17). The margins of regions of interest were marked on these strips of pixels (see Fig. 1) and the locations expressed as a percentage of the hemisphere position. For example, the #3 slice showed 34 pixels in the atlas from frontal midline to the posterior margin of the frontal lobe, 36 pixels in the parietal lobe and 19 in the occipital lobe, for a total of 89 pixels. The frontal lobe then extended from 1 to 38% of the perimeter (34/89). The 324 PET slice images were then sorted to match the levels in the atlas by one of us blind to the sleep stage (E.H.). The percentages were applied to each PET image similarly outlined, and the mean glucose metabolic rate across each sector

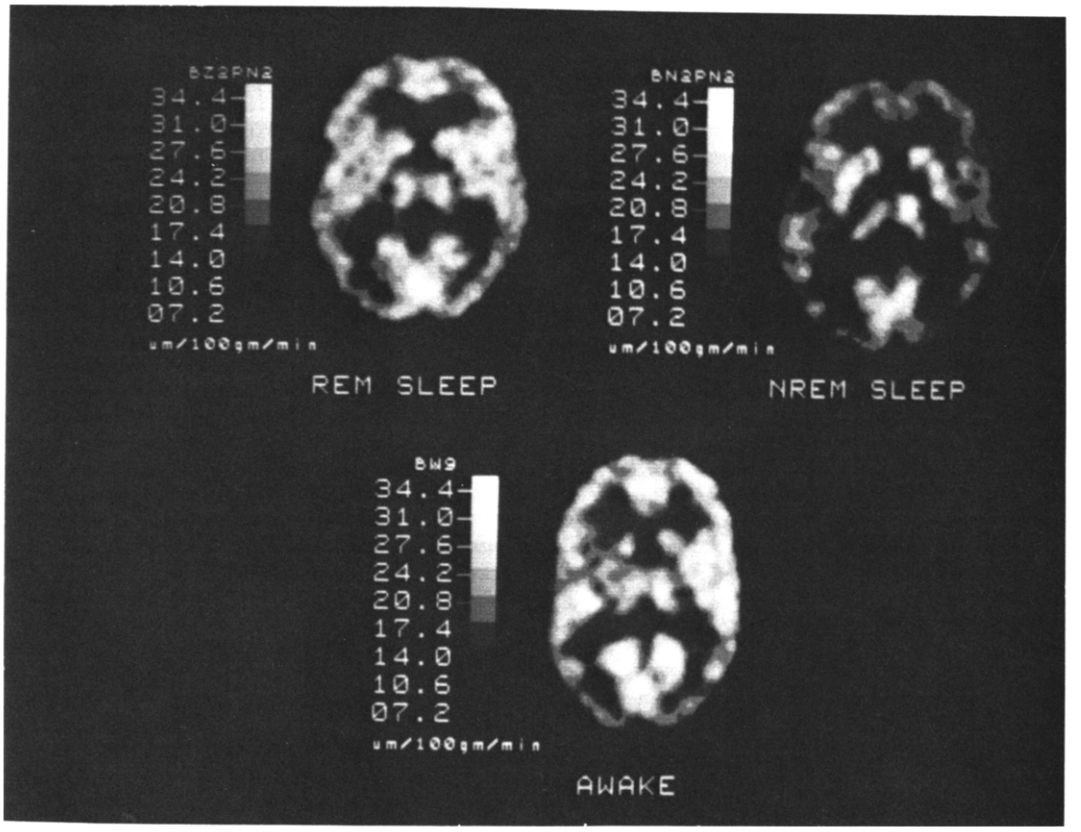

FIG. 2

Pet scans at midventricular level (#8, 41% of head height above the canthomeatal line) show overall decrease in metabolic rate in NREM sleep and right basal ganglia elevation in REM sleep. Scale bar is in metabolic rate in micromoles glucose/100g/min.

calculated (averaged over the pixels falling within these limits). Metabolic rates for cortical areas falling across more than one slice were calculated as the weighted average of the number of pixels contributing from each slice.

Subcortical areas were measured using the same atlas and a stereotaxic atlas method as described elsewhere (16).
Regions of interest were analyzed as mean metabolic rate for all structures. Values were also expressed as relative metabolic rate for the cortex as metabolic rate/whole brain metabolic rate, and for subcortical regions of interest as metabolic rate/whole slice metabolic rate.

We entered cortical metabolic rate values into a three-way ANOVA (19) with independent groups (awake, REM and NREM), hemisphere (left, right) and brain lobe (frontal, parietal, temporal, and occipital). Huynh-Feldt corrected df were used to correct for inflated degrees of freedom due to repeated measures with BMDP 4V (19). NREM sleep (mean 14.0, SD=3.7 micromoles/100g/min) showed a marked decrease in metabolic rate (Figure 2) compared with waking (21.4 $\pm$6.3) and REM (19.2 $\pm$4.3). This was confirmed with a main effect of group ($F=9.0$, d.f.=2,31, $p=0.0008$). The decrease with NREM was relatively greater in the frontal and temporal lobes (Table 1) and less in the temporal lobes (lobe by sleep stage group interaction, $F=3.25$, d.f.=2.77, 42.9, $p=0.03$). While the right hemisphere had higher metabolic rate than the left ($F=20.6$, $p=0.0001$), no interaction between sleep stage and hemisphere reached significance.

We also contrasted (Table 1) three major divisions of brain areas: the cortex (frontal, temporal, parietal, and occipital), the central gray matter (caudate, anterior and posterior putamen, thalamus, and globus pallidus), and the medial frontal cortex (medial frontal, cingulate cortex, anterior, middle, and posterior). The analysis was a four-way ANOVA with sleep stage groups as an independent groups factor and brain region (cortex, basal ganglia, medial cortex), hemisphere (left, right) and brain subregion (four areas within each main region) as repeated measures factors. Lower metabolic rates in NREM across all structures and significant regional differences in the effect of sleep stage were statistically confirmed with interactions for sleep stage by group and sleep stage by brain region by subregion (Table). Examination of table means revealed that the largest decrease with NREM was the medial frontal cortex (10.5 micromoles or 38.2% decrease from waking) and the smallest was the putamen (7.5 micromoles or 28.4%). Post-hoc t-tests revealed all regions were lower in NREM than awake ($p<0.05$) and all regions except the thalamus were lower in NREM than REM. The thalamus was the only area which was significantly lower in REM than awake. We also obtained a significant four-way interaction including hemisphere ($F=2.51$, df=11.1, 171, $p=0.0059$). This multiway interaction resulted from a greater left than right metabolic rate in REM but a greater right than left metabolic rate in NREM and awake for the cingulum and medial frontal regions; a loss of the normal waking right>left pattern was also seen in temporal cortex and the thalamus in REM.

On an exploratory basis, we examined the percentage change of each of 63 structures in the medial cortical and subcortical regions

in NREM and REM from waking. This revealed that the largest decreases during NREM (40-50%; t=3.15, p=0.005) were in the medial frontal region, the corpus callosum, the posterior thalamus and the frontal white matter. The smallest changes (20%; p=ns) were in the cerebellum, anterior and medial cingulate gyrus and frontal white matter. While most areas of the brain were lower in metabolic rate during REM than awake, the cingulate gyrus, corpus callosum, and optic radiations were higher although not significantly by t-test.

These present results in man, using the FDG PET technique, which demonstrate significantly reduced local cerebral glucose use in most areas during NREM sleep compared with wakefulness, are consistent with preliminary PET reports in man (13,14), with 2-deoxy- glucose methods in monkeys (10) and with some (20) but not all (21) studies in cats. Decreased metabolic rate in NREM sleep has also been inferred from human studies of cerebral blood flow

MEAN GLUCOSE METABOLIC RATE IN HUMAN SLEEP
(micromoles/100g/min)

Cortical area	Sleep Stage Awake (n=10) mean	SD	NREM (n=12) mean	SD	REM (n=12) mean	SD
Lateral cortex						
Frontal	23.5	6.5	15.1	4.2	20.8	4.0
Parietal	23.2	6.5	14.5	4.6	20.6	3.9
Temporal	17.6	4.6	12.2	3.1	16.0	3.8
Occipital	21.1	5.9	14.3	4.0	19.4	3.7
Mean	21.4	6.3	14.0	4.1	19.2	3.9
Subcortical gray						
Caudate	25.4	6.4	18.1	4.0	22.3	4.6
Putamen	26.4	6.8	18.9	4.7	23.4	4.9
Thalamus	24.3	7.2	15.6	4.4	18.2	3.8
Globus pallidus	22.7	6.0	16.2	3.5	20.3	4.8
Mean	24.7	6.6	17.2	4.3	21.1	4.9
Medial cortex						
Medial frontal	27.5	7.1	17.0	5.1	24.0	5.1
Anterior cing.	20.5	5.2	14.5	4.2	20.3	4.3
Mid. cing	19.8	5.0	13.4	3.8	18.9	4.1
Post. cing.	19.7	5.0	13.3	3.2	19.2	3.1
Mean	21.9	6.6	14.6	4.3	20.6	4.6
Grand Mean	22.6	4.5	15.3	4.4	20.3	4.5

Entire table ANOVA, sleep stage group effect, F=8.74, d.f.=2,31, p=0.001; group by brain region by subregion, F=3.68, df=8.7, 134, p=0.004; group by brain region by subregion by hemisphere, F=2.51, df=11.1, 171, p=0.0059. Group by brain region (lateral cortical/medial cortical/subcortical), F=2.33, df=3.1,47.5, p=0.08. Main effects of position (F=18.3), structure (F=59.0) and hemisphere (data not shown, F=48.2) were all highly significant (p<0.001).

IV lines failed to be patent for blood drawing on two awake subjects, so sample size for absolute metabolic rate is 10 for this group.

using 133-Xenon (22). The reduction in whole brain metabolic rate during NREM in man (23%) is somewhat less than that we reported in monkeys (35%), but both estimates reflect substantial changes which are probably greater than any other normal, behaviorally induced alterations in brain metabolism. In contrast to NREM sleep, REM sleep showed only a small increase in metabolic rate, in the same direction reported in earlier PET (13,14) and cerebral blood flow (22,23) reports. No specific "sleep centers" were identified in this study, but it is likely that reduced metabolic activity observed during NREM in midbrain and thalamus reflects decreased tonic activating influences from mesencephalon to medial and intralaminar thalamus.

The underlying physiological mechanism responsible for glucose metabolic rate, while not completely known, appears to reflect changes in energy requirements to maintain ionic gradients and recently postulated nonoxidative glucose consumption during focal neural activity (24). The sleep associated changes in local glucose matabolism generally parallel the results of single cell activity which usually decrease during NREM sleep and increase during REM sleep in most areas of brain (25). The present results are consistent with the "rest" theory of NREM sleep and demonstrate that REM or dreaming sleep is an activated state with a different pattern of brain activation than waking.

Acknowledgments

This work was supported by grants from the National Institute of Mental Health (MH41282,38738), the UCSD Mental Health Clinical Research Center (MH30914), the UCSD Fellowship in Clinical Psychopharmacology and Psychobiology (MH18339) and by the Veterans Administration Medical Service. We thank Deborah Herrera, Rick Storch, Carolyn Ruiz, Laura Sutton, and David Naimee for their technical assistance.

References

1. P.J. SHIROMANI, J.C. GILLIN, and S. HENRICKSEN, Ann. Rev. Pharmacol. Toxicol. 27 137-156 (1987).
2. R.T. WILKINSON, in O.G. Edholm and A.L. Bacharach (eds.) The Physiology of Human Survival, Academic Press, London, 399-430 (1965); P. NAITOH, R. PASNAU, and E.J. KOELLER, Biological Psychiatry 3 309-320 (1971).
3. W.B. WEBB, The Functions of Sleep (Academic Press, New York, NY, 1979).
4. R. MEDDIS, Animal Behavior, 23 676-691 (1975).
5. J. A. HORNE, Physiol. Psychol. 5 403-408 (1977).
6. F. SNYDER, Am. J. Psychiat. 123 121-136 (1966); E. HARTMANN, The Functions of Sleep, Yale University Press, New Haven, (1973).
7. H. ZEPLIN and A. RECHTSCHAFFEN, Brain and Behavioral Evolution 10 425-470 (1974).
8. J. HORNE, Why We Sleep, Oxford University Press, New York (1988).
9. R. J. BERGER, Fed. Proceedings 34 97-110 (1975).
10. C. KENNEDY, J. C. GILLIN, W.B. MENDELSON, S. SUDA, M. MIYAOKA, M. ITO, R.K. NAKAMURA, F.I. STORCH, K. PETTIGREW, M. MISHKIN, and L. SOKOLOFF. Nature 297

325-326 (1982).
11. A. RECHTSCHAFFEN, M. GUILAND, M.A. BERGMAN, and M. BERNARD, Science 221 182-184 (1983).
12. K. ADAM, Prog. Brain Res. 53 289-305 (1980); G. MORRUZZI and G. ERGEBNISSE, Physiol. 64 1 (1972).
13. W.-D. HEISS, G. PAWLIK, K. HERHOLZ, R. WAGNER, and K. WIENHARD, Brain Res. 327 362-366 (1985).
14. G. FRANCK, E. SALMON, R. POIRRIER, B. SADZOT, and G. FRANCO, Rev. EEG Neurophysiol. Clin. 17 71-77 (1987).
15. M.S. BUCHSBAUM, J.C. WU, R.J. HAIER, E. HAZLETT, R. BALL, M. KATZ, K. SOKOLSKI, M. LAGUNAS-SOLAR, and D.H. LANGER, Life Sciences 40 2393-2400 (1987).
16. M.S. BUCHSBAUM, H.H. HOLCOMB, L.E. DELISI, J.CAPPELLETTI, A.C. KING, J. JOHNSON, E. HAZLETT, R.M. POST, J. MORIHISA, W. CARPENTER, R. COHEN, D.PICKAR, and R. KESSLER, Arch. Gen. Psych. 41 1159-1166 (1984).
17. T. MATSUI and A. HIRANO, An Atlas of the Human Brain for Computerized Tomography, Igaku-Shoin, Tokyo, Japan (1978).
18. M.S. BUCHSBAUM, A.F. MIRSKY, L.E. DELISI, J. MORIHISA, C.N. KARSON, W.B. MENDELSON, A.C. KING, J. JOHNSON, and R. KESSLER, Psychiat. Res. 13 95-108 (1984).
19. W.J. DIXON, BMD Biomedical Computer Programs, University of California Press, Berkeley, CA (1982).
20. M. LIVINGSTON and D.H. HUBEL, Nature 291 554-561 (1981).
21. P. BOBILLIER, S. SEGUIN, F. PETITJEAN, C. BUDA, D. SALVERT, M. JANIN, G. CHOUVET, M. JOUVET, and M.H. DES ROSIERS, Brain Res. 240 359-363 (1982).
22. R.E. TOWNSEND, P. PRINZ, N. OBRIST, and D. WALTER, J. Applied Physiol. 35 620-625 (1973); F. SAKAI, J.S. MEYER, I. KARACAN, S. DERMAN, and M. YAMAMOTO, Ann. Neurol. 7 471-478 (1980).
23. M. REIVICH, G. ISAACS, E. EVARTS, and S. KETY, Trans Am. Neurol. Assoc. 92 70-74 (1967).
24. P.T. FOX, M.E. RAICHLE, M.S. MINTURN, and C. DENCE, Science 241 462-464 (1988).
25. M. STERIADE and J.A. HOBSON, Progress in Neurobiology 6 155-376 (1976).